2026 IEEE/SICE International Symposium on System Integration (SII)
January 11-14, 2026. Cancún, México

Incentive-Driven Energy Management System for Promoting EV User Cooperation*

Riho Hoshuyama[1] and Masaki Inoue[2]

Abstract— **In this paper, we address the design of an energy management system (EMS) that incorporates a mechanism to promote the cooperation of electric vehicle (EV) users. The proposed EMS incentivizes EV users to cooperate, particularly to remain at home and make their EVs available for discharging power to the grid as reserve capacity. To this end, we model the behavioral change of EV users in response to incentives. Then, we formulate model-based incentive-driven EMS (ID-EMS) design as an optimization problem and derive its analytic solution. Finally, we validate the effectiveness of the ID-EMS through numerical experiments. The experiments leverage real-world data on daily vehicle usage patterns and survey-based insights into user behavioral changes.**

I. INTRODUCTION

Smart grids, which are power grids that utilize information technology to optimize both power demand and supply, are attracting increasing attention. Effective management on both sides is expected to facilitate the large-scale integration of renewable energy into the grid, despite its inherent variability and uncertainty. In particular, recent works on smart grids have focused primarily on demand-side management and control technologies (see works [1]–[3] and references therein for further details).

A promising approach to demand-side management is the integration and coordination of electric vehicles (EVs). EV storage batteries are expected to be an alternative to large-scale energy storage systems. However, it is essential to ensure that their primary function, providing mobility, is not compromised. Integrating EVs into an energy management system (EMS) poses challenges in designing strategies that effectively incorporate EVs into the grid while maintaining user convenience and preferences.

To address these challenges, extensive research has been conducted on integrating EVs into EMSs, particularly focusing on the design of optimal charging strategies [4]–[7]. For example, the work [4] presents a reinforcement learning (RL)–based charging navigation framework that jointly considers both power system and traffic conditions. The work [5] proposes a generalized Nash game approach that minimizes individual charging costs for EVs. Fairness among EVs is achieved through Nash equilibrium, while uncertainties in renewable generation and aggregator capacity are explicitly considered. Beyond charging schedule optimization, several works [8], [9] address dynamic pricing mechanisms to regulate EV charging demand.

In addition to the works on prediction of EV demand and EV charging control, several works [10]–[16] have investigated the discharging control of EVs to the grid. Such Vehicle-to-Grid (V2G) technology has attracted considerable attention as an effective means of utilizing energy storage. For instance, the work [10] applies RL to optimize distribution grid operations while considering EV profitability, including battery health and mobility constraints during discharging. The work [11] analyzes the state-of-charge profiles of EV batteries during charging and discharging using iterative learning control for office workers with patterned commuting behavior. The work [12] addresses the optimal scheduling of EV charging and discharging in cyber–physical social systems. It aims to balance grid stability and user satisfaction by employing a moving-horizon approach to capture the stochasticity of EV mobility. Most works on V2G assume that EV users behave cooperatively with the EMS and make rational decisions. However, in practice, user participation in V2G operations depends on individual preferences and situational factors, introducing inherent uncertainty in human decision-making that must be considered in EMS design. Some works [8], [10], [12] have attempted to incorporate such behavioral uncertainty into energy allocation or pricing mechanisms, yet they still presuppose that EV users are already willing to cooperate with the EMS.

This paper focuses on a more fundamental issue—the willingness of EV users to cooperate with the EMS, rather than the design of their charging and discharging profiles. To foster user cooperation, this study adopts a behavioral economics perspective and employs monetary incentives as a management mechanism. The decision-making behavior of EV users in response to incentives is modeled using human-subject data collected through crowd-sourced questionnaires. Based on this model, an EMS with an incentive mechanism is formulated, and its analytical solution is derived. Finally, numerical simulations using real-world daily mobility data are conducted to verify the effectiveness of the proposed incentive-driven EMS (ID-EMS).

II. ID-EMS PROMOTING EV USERS COOPERATION

A. Overall Structure of ID-EMS

The flow of the proposed ID-EMS is illustrated in Fig. 1. The aggregator, which acts as an intermediary between

*This work was supported by Grant-in-Aid for Scientific Research (B), No. 25K01254 JSPS

[1]Riho Hoshuyama is with the Department of Applied Physics and Physico-Informatics, Keio University, Yokohama, Japan riho_hoshu@keio.jp

[2]Masaki Inoue is with the Department of Applied Physics and Physico-Informatics, Keio University, Yokohama, Japan minoue@appi.keio.ac.jp

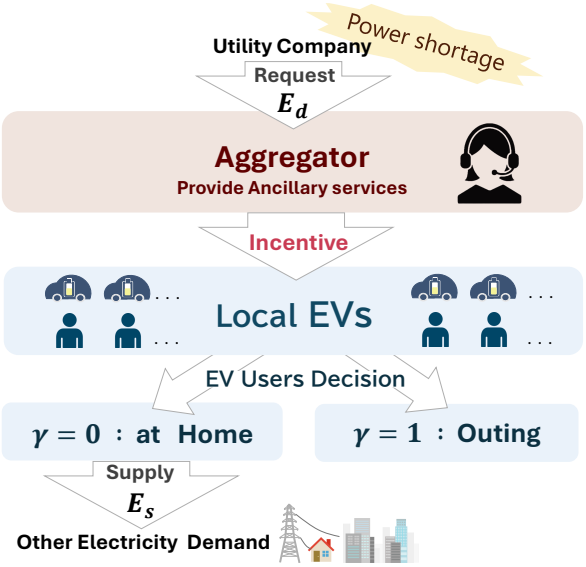

Fig. 1. Overall structure of ID-EMS

utility companies and EV users, provides ancillary services by securing reserve capacity during power shortages. As a profit-oriented entity, the aggregator offers a subscription-based service to EV users. In return for cooperating with power supply, users receive bill discounts as incentives. When a power shortage is predicted within the grid, the utility company requests the aggregator to secure reserve capacity, denoted by E_d. The aggregator then manages its registered EVs through incentives to ensure that the total available power supply, denoted by E_s, exceeds E_d.

The state of an EV is represented by γ, where $\gamma = 0$ indicates that the EV is at home and available for discharging to the grid, while $\gamma = 1$ indicates that the EV is out and is not available. Assuming that EVs' charging and discharging occur only at home, any parking status other than at home is also categorized as $\gamma = 1$. Although the availability of EVs parked at home during the daytime is uncertain in contrast to commuter EVs with regular schedules, they remain priority targets in the EMS, as they are typically unused and retain substantial dischargeable energy. In this study, we assume that EV users decide between $\gamma = 0$ and $\gamma = 1$ in response to monetary incentives, and the aggregator aims to secure EVs in available state $\gamma = 0$.

The EV state at the time of the request is denoted by γ_0, and the number of EVs in state $\gamma_0 = 0$ is represented by X_0. These X_0 EVs serve as the potential power supply sources for the EMS. However, some of these EVs may depart during the supply period. To address this, the aggregator performs departure prediction of EVs, as described in Subsection II-B, and incentivizes EV users to encourage cooperation, as described in Subsection II-C. The design of ID-EMS, which integrates both prediction and incentive mechanisms, is formulated in Subsection II-D.

B. Modeling of EV State Prediction

Upon receiving a reserve capacity request, the aggregator first predicts the future states of EVs. This prediction is performed at the time of the request, defined as the initial time $k = 0$. The predicted state at time k is denoted by $\hat{\gamma}_k$ and is derived based on historical mobility data, the initial state γ_0, and the duration u_0 for which the initial state has been maintained. In this paper, the prediction is performed using the maximum-likelihood estimation based on previous work [17]. Consequently, the predicted state of each EV i at time k is described by

$$\hat{\gamma}_k^i = f(\gamma_0^i, u_0^i). \tag{1}$$

To integrate EV state predictions into the EMS, individual predictions $\hat{\gamma}_k^i$ are aggregated to estimate the total number of EVs available for reserve capacity, i.e. EVs at home. Let N denote the total number of registered EVs. Then, the proportion of EVs that were at home at the initial time $k = 0$ and predicted to remain at home at the time $k \in \{1, 2, \ldots, T\}$ is expressed as follows.

$$P = \sum_{i=1}^{N}(1 - \hat{\gamma}_k) / \sum_{i=1}^{N}(1 - \gamma_0^i). \tag{2}$$

Since the number of EVs with $\gamma_0 = 0$ is X_0, it follows that $\sum_{i=1}^{N}(1-\gamma_0^i) = X_0$. Therefore, the number of EVs expected to remain available at time k is expressed as $X_0 P$.

C. Modeling of Incentive-Driven Behavioral Change

In this subsection, we consider the case where the requested reserve capacity E_d is large and the total number of EVs available for reserve capacity described in Subsection II-B, $X_0 P$, is insufficient to meet the request. To address this shortfall, incentives are offered to EV users who are initially predicted to be unavailable, i.e., EVs with $\hat{\gamma}_k^i = 1$, to encourage them to stay home and cooperate with the power supply. This incentive mechanism aims to increase the number of available EVs, i.e., EVs with $\hat{\gamma}_k^i = 0$.

Let q denote the incentive offered to EV users. Then, the probability that an EV user initially scheduled to be out, which means $\hat{\gamma}_k^i = 1$, changes their behavior and remains at home, which means $\hat{\gamma}_k^i = 0$, is modeled as

$$\Delta P(q) = \beta_1 q^2 + \beta_2 q, \tag{3}$$

where β_1 and β_2 are positive constants. The function is derived from empirical data collected through a questionnaire survey. The details of the data collection and modeling procedure are provided in Subsection **??**.

Note that $\Delta P(0) = 0$, as the incentive-driven behavior change only targets users predicted to be unavailable. The coefficients β_1 and β_2 are assumed to be positive, ensuring that the function in (3) is convex and monotonically increasing for the positive incentive value of q.

D. Incentive-Driven EMS

With the foundations established in the previous subsections, we proceed to formulate the ID-EMS. The EMS aims to (i) secure the requested reserve capacity E_d through incentive-based cooperation of EV users, and (ii) minimize the total incentive payment. Using the prediction models given in (2) and (3), ID-EMS is formulated as follows.

Problem 1. *Given E_d, ϵ, P, $\Delta P(\cdot)$, X_0, and $q_{\max}$, solve the following optimization problem*

$$\min_{q,X} \quad qX \tag{4a}$$

$$\text{sub to} \quad E_s = \epsilon\{XP + \Delta P(q)X(1-P)\} \tag{4b}$$

$$E_d \le E_s \tag{4c}$$

$$0 \le X \le X_0 \tag{4d}$$

$$0 \le q \le q_{\max} \tag{4e}$$

In this formulation, the aggregator determines the amount of incentive q to offer to EV users and the number of EVs to request, denoted by X. Let (q^*, X^*) be the optimal solution to Problem 1, which minimizes the total incentive cost while satisfying the required reserve capacity. Although q and x are discrete in practical applications, they are treated here as continuous variables to allow a tractable optimization formulation.

The constraints of Problem 1 are explained below. Constraint (4b) estimates the total power supplied by cooperative EVs, denoted by E_s. Among the requested X EVs, XP are expected to be available without incentives, while $X(1-P)$ are initially unavailable. Multiplying $X(1-P)$ by $\Delta P(q)$ gives the expected number of additional EVs that became available due to incentives. Thus, the total expected number of available EVs is $XP + \Delta P(q)X(1-P)$. Multiplying this quantity by the per-EV supply ϵ, representing the power contributed by each EV, yields E_s. Constraint (4c) ensures that the estimated total supply E_s exceeds the requested E_d. Finally, constraints (4d) and (4e) specify the feasible ranges for the decision variables X and q, respectively.

Remark 1. *In Problem 1, the value of P inevitably contains some uncertainty and, therefore, the problem formulation is extended accordingly. Suppose that the confidence level of R is available for the value P. Then, the total power supply E_s is estimated using the following model instead of (4b).*

$$E_s = \epsilon[XPR + X(1-P)(1-R) + \Delta P(q)\{X - X\{PR + (1-P)(1-R)\}\}]. \tag{5}$$

We see that if the confidence level is set to $R = 1$, (5) is reduced to $\epsilon\{XP + \Delta P(q)X(1-P)\}$, which is the same as (4b). In this sense, the extended model (5) presents a generalization that accounts for the uncertainty in the prediction of P.

E. Analysis of the ID-EMS

Problem 1 belongs to the class of nonconvex optimization problems, and therefore, the existence and uniqueness of the solution are not trivial. In this subsection, we analyze Problem 1 to derive its analytic solution.

To simplify the description of Problem 1, we let

$$P_{\text{all}}(q) := P + \Delta P(q)(1-P). \tag{6}$$

By (4b) and (4c), we obtain $E_d \le \epsilon X P_{\text{all}}(q)$. Since $P_{\text{all}}(q)$ increases monotonically, the optimal solution (q^*, X^*) must satisfy the equality $X = E_d/\epsilon P_{\text{all}}(q)$. Eliminating X using this equality simplifies all conditions, and Problem 1 is reduced to the following problem.

Problem 2. *Given E_d, ϵ, $P_{\text{all}}(\cdot)$, X_0, and $q_{\max}$, solve the following optimization problem*

$$\min_{q} \quad \frac{q}{P_{\text{all}}(q)} \tag{7a}$$

$$\text{sub to} \quad \frac{E_d}{\epsilon X_0} \le P_{\text{all}}(q) \tag{7b}$$

$$0 \le q \le q_{\max} \tag{7c}$$

To solve the problem, we first estimate the feasible region of q by expanding the inequality (7b). Recall that $P_{\text{all}}(q)$ is increasing monotonically. Noting $P_{\text{all}}(0) = P$, the inequality implies $0 \le q$ if $\frac{E_d}{\epsilon X_0} \le P$, otherwise $q_{\text{lim}} \le q$ if $P < \frac{E_d}{\epsilon X_0}$, where q_{lim} satisfies

$$P_{\text{all}}(q_{\text{lim}}) = \frac{E_d}{\epsilon X_0}. \tag{8}$$

Recalling $P_{\text{all}}(q)$ from (6), ΔP from (3), and (7c), we explicitly express q_{lim} to derive the following lemma.

Lemma 1. *The feasible region of q in Problem 2 is expressed as follows.*

$$q_{\text{lim}} \le q \le q_{\max},$$

where q_{lim} is the constant satisfying

$$q_{\text{lim}} = \begin{cases} 0 & if \frac{E_d}{\epsilon X_0} \le P, \\ -\frac{\beta_2}{2\beta_1} + \frac{1}{\beta_1}\sqrt{\frac{E_d\beta_1 - \epsilon X_0(\beta_1 P + {\beta_2}^2 - {\beta_2}^2 P)}{\epsilon X_0(1-P)}} & \\ & if \frac{E_d}{\epsilon X_0} > P. \end{cases} \tag{9}$$

The lemma provides the explicit lower and upper bounds of q. Next, we estimate the value range of the objective function given in (7a). To simplify the description of Problem 2, we let

$$Q(q) := \frac{q}{P_{\text{all}}(q)}. \tag{10}$$

It follows from (6) and (3) that

$$Q(q) = \frac{q}{(1-P)\beta_1 q^2 + (1-P)\beta_2 q + P}. \tag{11}$$

Note that $\frac{dQ(q)}{dq} = \frac{-\beta_1(1-P)q^2 + P}{\{\beta_1(1-P)q^2 + \beta_2(1-P)q + P\}^2}$, and its denominator $\{\beta_1(1-P)q^2 + \beta_2(1-P)q + P\}^2$ is positive for all q. Then, based on the shape of the numerator $-\beta_1(1-P)q^2 + P$, we see that $Q(q)$ is concave and takes the peak value at $q = \sqrt{\frac{P}{\beta_1(1-P)}}$. By summarizing the discussion in this paragraph, we have the following lemma.

Lemma 2. *The objective function in (11) is concave and attains its peak value at*

$$q = q_{\text{peak}} := \sqrt{\frac{1}{\beta_1}\frac{P}{1-P}}. \tag{12}$$

From Lemmas 1 and 2, we see that the solution to Problem 2 is the lower limit or the maximum value, denoted by q_{lim} or $q_{\max}$, respectively, depending on the values of q_{lim}, q_{peak}, and $q_{\max}$. Suppose that the resulting solution to the problem, denoted by q^*, is given in the following theorem.

Theorem 1. *The solution to Problem 1, (q^*, X^*), is given by*

$$q^* = \begin{cases} \textit{No solution} & \textit{if } \ q_{\text{lim}} > q_{\max}, \\ q_{\max} & \textit{if } \ q_{\text{peak}} \le q_{\text{lim}} \le q_{\max}, \\ \underset{q \in \{q_{\text{lim}},\ q_{\max}\}}{\operatorname{argmin}} \ Q(q) & \textit{if } \ q_{\text{lim}} \le q_{\text{peak}} \le q_{\max}, \\ q_{\text{lim}} & \textit{if } \ q_{\text{lim}} \le q_{\max} \le q_{\text{peak}} \end{cases} \tag{13}$$

and $X^* = E_d/\epsilon P_{\text{all}}(q^*)$.

The theorem presents the analytic solution to Problem 1, which serves as the core management logic of ID-EMS. In the practical operation of ID-EMS, the aggregator observes X_0 and estimates P to determine the optimal solution (q^*, X^*), which specifies the incentives and the corresponding number of cooperative EV users.

We first consider the case where the requested E_d is excessively large relative to the number of available EVs X_0 and the estimated rate P. This implies that q_{lim} defined in (9) becomes so large that q^* does not exist. This corresponds to a "No solution" case, indicating that the required reserve capacity cannot be secured, regardless of the incentive offered. Next, we consider the case where E_d is relatively small compared to X_0 and P, such that $q^* = q_{\text{lim}}$. In particular, we further assume that E_d is sufficiently small, Lemma 1 and Theorem 1 show that $q^* = q_{\text{lim}} = 0$, indicating that no incentives are necessary to secure the requested reserve capacity. Finally, when E_d and P are finely balanced, Theorem 1 plays an essential role in determining incentives and the number of cooperative EV users.

III. NUMERICAL EXPERIMENTS

In this section, we conduct numerical experiments as the ID-EMS aggregator presented in Section II. Through experiments, we demonstrate the effectiveness of ID-EMS in various scenarios.

As a preliminary, data-driven modeling of the behavioral change of EV users is addressed based on human-subject data collected through crowd-sourced questionnaires[1]. 1000 participants were asked how many incentives they would require delaying their scheduled outing and comply with a stay-at-home request. The results are shown in Fig. 2. The six colors each represent a response in a different situation. Fitting these obtained data into the form of (3) resulted in the model as follows.

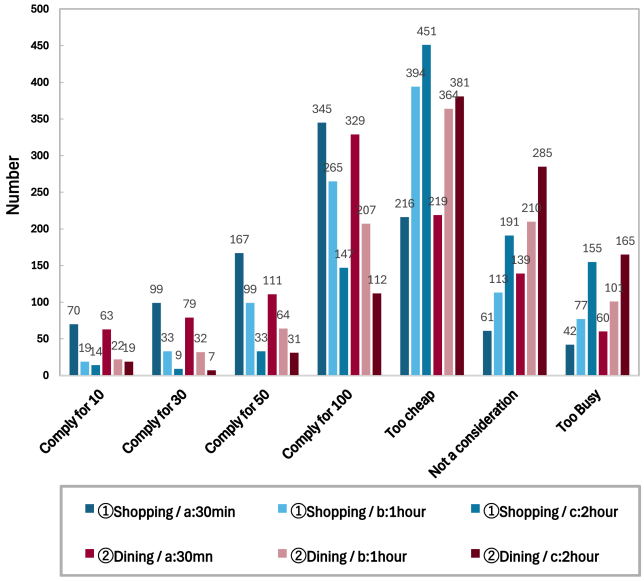

Fig. 2. Survey Results

$$\Delta P(q) = 0.0016q^2 + 0.2377q. \tag{14}$$

Using the model (14), we present the results of numerical experiments on ID-EMS, stated in Section II.

To set up various scenarios, we utilized open data on car usage given in [18]. The usage data of ten cars were virtually expanded to 100 cars each, setting up numerical simulations with a total of 1,000 registered EVs. Since power shortages tend to occur during the daytime when power consumption is particularly high, the initial time $k = 0$ was set randomly between 11:00 and 15:00. The waiting time for supply was fixed at 1 hour and the date was set randomly.

The parameters used in ID-EMS, stated in Problem 1, were set as follows. First, we let $\epsilon = 30$ kWh, representing half of the maximum energy storage capacity of commercially available EVs. In addition, we let $E_d \in \{1000, 1100, 1200, \cdots, 30000\}$ kWh. The minimum value of 1000 kWh was determined to be the minimum that would cause a power request to be issued. The maximum value of 30,000 kWh was the maximum amount supplied by 1000 EVs per $\epsilon = 30$ kWh. The ID-EMS, formulated as in Problem 1, was extended to incorporate the confidence level of prediction and regularization, as described in Remarks 1. In particular, we set $R = 0.8$ based on prediction experiments and $\alpha = 0.01$.

Although Subsection II-E presented an analytical solution for determining the incentive q in the ID-EMS formulation, the modified setting with elements such as prediction confidence and regularization makes the optimization problem more complex. Specifically, the definition of P_{all} differs from

[1]Informed consent was obtained from participants before the experiment. Specifically, participants were informed that their responses would be used solely for research purposes and that the results could be published, and their consent was obtained accordingly.

TABLE I

RESULT OF NUMERAL EXPERIMENTS

Scenario	given value	predicted value		solution	
	E_d [kWh]	X_0 [units]	P	q [JPY]	X [units]
1	2700	300	$0.\dot{6}$	0	225
2	5400	300	$0.\dot{6}$	89	300
3	19000	800	1	0	792
4	17000	800	0.714	64	800
5	17000	600	1	unable to cover	

that in (6), resulting in a different solution for $q_{\lim}$ in (9) and q_{peak} in (12). However, since the utility function $Q(q)$ retains a similar overall shape, both $q_{\lim}$ and q_{peak} can be computed numerically, and an analytical solution similar to that presented in Theorem 1 can be derived accordingly. In particular, considering the definition of $\Delta P(q)$ in (14) and the associated parameter settings described above, the calculated q_{peak} exceeds the maximum allowable incentive $q_{\max}$. Therefore, among the four candidate solutions described in Theorem 1, only two possibilities remain: "No Solution" when the required reserve cannot be secured, or the lower bound $q_{\lim}$ when the reserve requirement is satisfied without exceeding the incentive limit.

Table I shows the results of numerical experiments performed in five different scenarios. Scenarios 1 and 2 assume that the requested reserve capacity E_d was relatively small. The experimental results indicate that as the requested E_d increases from Scenario 1 to Scenario 2, the incentive q for EV users became necessary. The resulting values of q closely align with the theoretical $q_{\lim}$. Scenarios 3 to 5 correspond to a large-scale EMS, where the initial number of EVs available for supply X_0 and the predicted supply availability proportion P vary. In Scenario 3, although it has the largest E_d, the reserve power capacity is secured without any incentive. In contrast, Scenarios 4 and 5 have a small number of EVs available for supply, resulting in different outcomes: in Scenario 4, reserve capacity E_d was secured through incentives, while in Scenario 5, the limited incentives were insufficient to secure the requested E_d, leading to the case of "No solution". These results indicate that not only requested E_d but also the number of available EVs X_0 and the proportion of availability P, which depends on EV state prediction stated in Subsection II-B, significantly affect the results of X and q.

In all scenarios, proposed ID-EMS effectively manages registered EVs by utilizing incentives q in response to the real-time EV usage prediction $\hat{\gamma}_k^i$ and the requested reserve capacity E_d.

IV. CONCLUSION

In this paper, we designed an energy management system that utilizes a fleet of registered EVs as reserve power capacity. Models were developed to predict the behavior of EV users and their incentive-driven behavioral changes. Based on these models, a management strategy was formulated to support decision making. Further analysis of the management system led to a closed-form derivation of the management logic, formulated as a nonconvex optimization problem. Finally, we conducted numerical experiments of the proposed management system using human-subject data collected from crowd-sourced questionnaires and real-world car usage data.

REFERENCES

[1] "Demand side management: Benefits and challenges," *Energy Policy*, vol. 36, no. 12, pp. 4419–4426, 2008, foresight Sustainable Energy Management and the Built Environment Project.

[2] P. Samadi, H. Mohsenian-Rad, R. Schober, and V. W. S. Wong, "Advanced demand side management for the future smart grid using mechanism design," *IEEE Transactions on Smart Grid*, vol. 3, no. 3, pp. 1170–1180, 2012.

[3] "Demand response and smart grids—a survey," *Renewable and Sustainable Energy Reviews*, vol. 30, pp. 461–478, 2014.

[4] T. Qian, C. Shao, X. Wang, and M. Shahidehpour, "Deep reinforcement learning for ev charging navigation by coordinating smart grid and intelligent transportation system," *IEEE Transactions on Smart Grid*, vol. 11, no. 2, pp. 1714–1723, 2020.

[5] W. Wei, F. Liu, and S. Mei, "Charging strategies of ev aggregator under renewable generation and congestion: A normalized nash equilibrium approach," *IEEE Transactions on Smart Grid*, vol. 7, no. 3, pp. 1630–1641, 2016.

[6] C. B. Saner, A. Trivedi, and D. Srinivasan, "A cooperative hierarchical multi-agent system for ev charging scheduling in presence of multiple charging stations," *IEEE Transactions on Smart Grid*, vol. 13, no. 3, pp. 2218–2233, 2022.

[7] Y. Cao, T. Jiang, O. Kaiwartya, H. Sun, H. Zhou, and R. Wang, "Toward pre-empted ev charging recommendation through v2v-based reservation system," *IEEE Transactions on Systems, Man, and Cybernetics: Systems*, vol. 51, no. 5, pp. 3026–3039, 2021.

[8] C. Lu, J. Wu, J. Cui, Y. Xu, C. Wu, and M. C. Gonzalez, "Deadline differentiated dynamic ev charging price menu design," *IEEE Transactions on Smart Grid*, vol. 14, no. 1, pp. 502–516, 2023.

[9] T.-H. Huang, C.-S. Tai, and L.-C. Fu, "Demand response in residential and commercial community considering user comfort using improved particle swarm optimization," in *2018 IEEE International Conference on Systems, Man, and Cybernetics (SMC)*, 2018, pp. 1215–1220.

[10] J. Xie, P. Vorobev, R. Yang, and H. Dinh Nguyen, "Battery health-informed and policy-aware deep reinforcement learning for ev-facilitated distribution grid optimal policy," *IEEE Transactions on Smart Grid*, vol. 16, no. 1, pp. 704–717, 2025.

[11] D. H. Nguyen, "Iterative learning control design for iteration-varying state-of-charge profiles of electric vehicle batteries," *IEEE Transactions on Systems, Man, and Cybernetics: Systems*, vol. 55, no. 1, pp. 805–816, 2025.

[12] W. Li, Z. Lin, H. Zhou, and G. Yan, "Multi-objective optimization for cyber-physical-social systems: A case study of electric vehicles charging and discharging," *IEEE Access*, vol. 7, pp. 76 754–76 767, 2019.

[13] H. Li, Z. Wan, and H. He, "Constrained ev charging scheduling based on safe deep reinforcement learning," *IEEE Transactions on Smart Grid*, vol. 11, no. 3, pp. 2427–2439, 2020.

[14] P. Hou, G. Yang, J. Hu, and P. J. Douglass, "A network-constrained rolling transactive energy model for ev aggregators participating in balancing market," *IEEE Access*, vol. 8, pp. 47 720–47 729, 2020.

[15] S. Sun, M. Dong, and B. Liang, "Real-time welfare-maximizing regulation allocation in dynamic aggregator-evs system," *IEEE Transactions on Smart Grid*, vol. 5, no. 3, pp. 1397–1409, 2014.

[16] Z. Lei, C. Xiao, D. Jiang, and Z. Ao, "Multi-objective optimization and discrete action set based rolling optimal lookahead schedule for coordinating electric vehicles," in *2024 IEEE International Conference on Systems, Man, and Cybernetics (SMC)*, 2024, pp. 5200–5205.

[17] T. Yamaguchi, A. Kawashima, A. Ito, S. Inagaki, and T. S. and, "Real-time prediction for future profile of car travel based on statistical data and greedy algorithm," *SICE Journal of Control, Measurement, and System Integration*, vol. 8, no. 1, pp. 7–14, 2015.

[18] Nagoya University, "Nagoya University Open Data for EMS Evaluation," http://data.v2x-ems.nagoya/down/sample, accessed: 3 March 2025.